Cellular and Molecular Life Sciences

ORIGINAL ARTICLE

Distinct functions of Crumbs regulating slit diaphragms and endocytosis in *Drosophila* nephrocytes

Florian Hochapfel[1,2] · Lucia Denk[1] · Gudrun Mendl[1] · Ulf Schulze[2] ·
Christine Maaßen[1] · Yulia Zaytseva[1] · Hermann Pavenstädt[2] · Thomas Weide[2] ·
Reinhard Rachel[1] · Ralph Witzgall[1] · Michael P. Krahn[1,2]

Abstract   Mammalian podocytes, the key determinants of the kidney's filtration barrier, differentiate from columnar epithelial cells and several key determinants of apical–basal polarity in the conventional epithelia have been shown to regulate podocyte morphogenesis and function. However, little is known about the role of Crumbs, a conserved polarity regulator in many epithelia, for slit-diaphragm formation and podocyte function. In this study, we used *Drosophila* nephrocytes as model system for mammalian podocytes and identified a conserved function of Crumbs proteins for cellular morphogenesis, nephrocyte diaphragm assembly/maintenance, and endocytosis. Nephrocyte-specific knockdown of Crumbs results in disturbed nephrocyte diaphragm assembly/maintenance and decreased endocytosis, which can be rescued by *Drosophila* Crumbs as well as human Crumbs2 and Crumbs3, which were both expressed in human podocytes. In contrast to the extracellular domain, which facilitates nephrocyte diaphragm assembly/maintenance, the intracellular FERM-interaction motif of Crumbs is essential for regulating endocytosis. Moreover, Moesin, which binds to the FERM-binding domain of Crumbs, is essential for efficient endocytosis. Thus, we describe here a new mechanism of nephrocyte development and function, which is likely to be conserved in mammalian podocytes.

✉ Michael P. Krahn
   Michael.Krahn@ukmuenster.de

1   Molecular and Cellular Anatomy, University of Regensburg, Universitätsstr. 31, 93053 Regensburg, Germany

2   Medizinische Klinik und Poliklinik D, Universitätsklinikum Münster, Domagkstr. 3a, 48149 Münster, Germany

Introduction

In vertebrates, podocytes play a crucial role in the establishment of the filtration barrier. A dysfunction of these cells consequently leads to renal failure. During kidney development, podocytes acquire a highly specialized morphology, changing their shapes from columnar epithelial cells to an elaborated outstretched form with primary-, secondary-, and foot processes, which encompass the glomerular arterioles. Subsequently, the slit diaphragm, a highly organized structure composed of glycosylated transmembrane proteins and their intracellular adaptors, is established to regulate the filtration slit between the foot processes.

Beside its core components of podocyte-specific proteins (most importantly, the immunoglobulin-domain proteins Nephrin and Neph1 and the adaptor protein Podocin [1]), assembly of the slit diaphragm has been reported to depend on several proteins which localize to the Tight junctions (TJ) in conventional epithelia [2], e.g., *Zonula Occludens* protein 1 [3, 4], PARtitioning defective 3 [5], and atypical Protein Kinase C [5–9]. Thus, podocytes maintain their intrinsic apical–basal polarity while extending the apical domain [cell body and (foot) processes, facing the urinary space] and shrinking the basolateral plasma membrane (anchored on the glomerular basal membrane).

One key determinant of apical–basal polarity in many if not all epithelia is the transmembrane protein Crumbs (Crb). *Drosophila* Crb (DmCrb) functions together with PAR-3 (Bazooka in *Drosophila*) to determine the apical plasma membrane domain. Both complexes counterbalance the activity of the basolateral determinants lethal giant

larvae (Lgl), discs large (Dlg), and scribble (Scrib) [10]. Apart from one described exception in boundary cells of the hindgut [11], DmCrb has to be stabilized at the TJ (or the TJ-homologous region in *Drosophila* epithelia) by binding its adaptor protein Stardust (Sdt, Protein associated with Lin-7 one, Pals-1, in mammals) [12–16]. The third member of the canonical Crb complex, PATJ (Pals1-associated TJ protein), is not essential for stabilization of Crb–Sdt in epithelial cells of the embryonic epidermis but in photoreceptor cells and in cultured mammalian cells [17–22]. Loss of DmCrb results in disturbed apical–basal polarity and defects in adherens junction (AJ) formation [23].

In contrast to *Drosophila*, three genes encode Crb proteins in mammals: Expression of Crb1 is restricted to the nervous system (and testis), whereas Crb2 is present in kidney, testis, placenta, and cerebral cortex. Finally, Crb3 can be detected in many if not all epithelia (the human protein atlas [24]) [25]. Loss of Crb3 in mice has been recently described to be postnatal lethal, but the described defects in apical–basal polarity in epithelia are not as strong as seen for its *Drosophila* counterpart: For instance, the formation of TJ/AJ in the tubular system of the kidney is largely unaffected [26]. Apart from its function in the retina [27], there is little information about the molecular function of Crb2, although it resembles DmCrb regarding its protein domain structure and is thus likely the direct homologue in certain tissues. In contrast, Crb3 virtually lacks the extracellular domain (Fig. 1a). Crb2-deficient mice die in embryonic stages, displaying gastrulation defects [28]. Interestingly, mutations in Crb2 are found in patients suffering from nephrotic syndrome [29] or congenital nephrosis [30]. Moreover, loss of Crb2 in zebrafish results in defects in foot-process development and slit-diaphragm assembly [29, 31].

To further explore the function of Crb in podocytes, we used *Drosophila* nephrocytes as model system. Nephrocytes have been recently identified as podocyte-homologous cells exhibiting a striking similarity in morphology, protein expression, and function [32–35]: nephrocytes are more or less round, mono- (pericardial) or di- (garland) nucleated cells. They are floating in the larval and adult stage hemolymph in two populations: Garland nephrocytes surrounding the foregut and pericardial nephrocytes lining up on both sides of the heart tube. One hallmark of these cells is the formation of elongated infoldings of their plasma membrane. These structures resemble podocyte foot processes and are connected by a nephrocyte diaphragm at the most exterior part (Fig. 2g). Narrow lacunae are formed between the foot processes and the nephrocyte diaphragms seal this microcompartment towards the extracellular space. The nephrocyte diaphragm has been shown to be composed of similar proteins as the slit diaphragm in mammals (e.g., Nephrin, NEPH1, Podocin), exhibiting a size-selective barrier [32, 33]. Upon filtration of certain substances, presumably toxins

and metabolic wastes, from the hemolymph, these components are endocytosed and intracellularly stored.

In this study, we investigated the function of Crb in morphogenesis and function of nephrocytes. DmCrb localizes to the cell periphery and colocalizes with nephrocyte diaphragm markers. Knock-down of DmCrb results in a drastic decrease in filtration rate, disturbed morphology of foot processes, and reduced nephrocyte diaphragms. These defects can be rescued by introduction of RNAi-resistant DmCrb as well as by expression of each of its human homologues, which are expressed in mouse podocytes, hCrb2 or hCrb3. Notably, knock-down of Crb disturbs the accumulation of early and late endosomes, which can partly be rescued by simultaneous overexpression of Moesin, which binds to the FERM-binding domain of Crb. In contrast, the assembly or maintenance of nephrocyte diaphragms does not depend on the interaction with Moesin but on the extracellular domain.

Materials and methods

Drosophila stocks and genetics

Fly stocks were cultured on the standard cornmeal agar food and maintained at 25 °C. For evaluation of filtration efficiency, the nephrocyte-specific driver line *sns::GAL4* [33] was recombined with *mhc::*ANP–RFP [36] and subsequently crossed to the responder lines UAS::mCherry–RNAi (#35778), UAS::Sdt–RNAi#1 (#37510), UAS::Crb–RNAi#1 (#38373), UAS::PATJ–RNAi (#35747), UAS::Yrt–RNAi (#36118), UAS::Ex–RNAi (#34968) (Bloomington Stock Center, Bloomington, IL, USA), UAS::Sdt–RNAi#2 (#15342R-2), UAS::PATJ–RNAi#2 (#12021R-4) (National Institute of Genetics, Shizuoka, Japan), UAS::Moesin–RNAi (#110654), and UAS::Crb–RNAi#2 (#22076) (Vienna *Drosophila* Resource Center, Austria). For rescue experiments, *sns::GAL4, mhc::*ANP–RFP was recombined with *UAS::Crb–RNAi#1*. The 21 nucleotide targeting sequence of Crb–RNAi#1 is located in the 3′ UTR of Crb mRNA, and thus, expression of this shRNA downregulates endogenous Crb but not Crb expressed from UASt as all constructs used in this study lack the 3′ UTR. The following stocks were established in this study using Phi-C31-integrase system [37] with attP40 (25C) and attPVK00002 (28E): UASt::DmCrb, UASt::DmCrb$_{\Delta FERM}$ [Y10A, E16A, 38], UASt::DmCrb$_{\Delta ERLI}$, UASt::DmCrb$_{\Delta intra}$, UASt::DmCrb$_{intra}$, UASt::DmCrb$_{intra\Delta ERLI}$, UASt::GFP–hCrb2, UASt::GFP–hCrb2$_{\Delta ERLI}$, UASt::GFP–hCrb2$_{\Delta FERM}$, UASt::GFP–hCrb2$_{C620S}$, UASt::GFP–hCrb2$_{C633W}$, UASt::GFP–hCrb2$_{R1249Q}$, UASt::GFP–hCrb3a, UASt::GFP–hCrb3a$_{\Delta ERLI}$, UASt::GFP–hCrb3b, and UASt::GFP–hCrb3b$_{\Delta CLPI}$. For
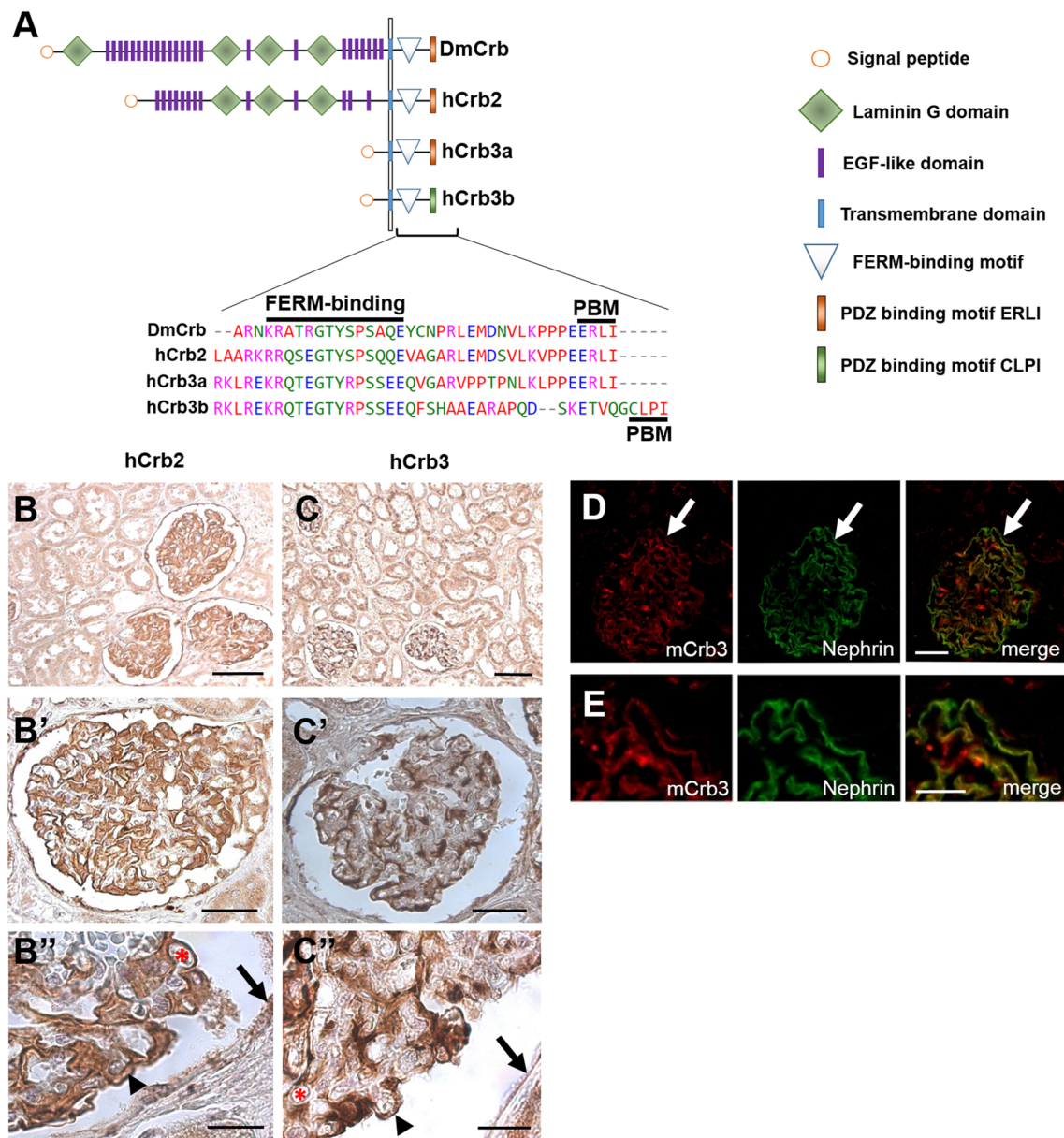
Fig. 1 Crb2 and Crb3 are expressed in human podocytes. **a** Scheme of *Drosophila* Crb and hCrb2 and hCrb3 proteins including a sequence alignment of the intracellular domain. *PBM* PDZ-binding motif, *FERM* 4.1-protein–Ezrin–Radixin–Moesin. **b, c** Immunostainings of human kidney sections (cortex). Note that hCrb2 expression is prominent in glomeruli [podocytes (*arrow head*), endothelial cells (*asterisk*), and parietal cells (*arrow*) in **b″** and **c″**] but only faint in tubules, whereas hCrb3 is strongly expressed in both glomeruli and tubules (**c**). **d** Mouse Crb3 colocalizes with mouse Nephrin in glomeruli of kidney sections of an adult mouse (3 months). **e** Magnification of the *arrow*-marked area is shown in the *right panels*. *Scale bars* 100 µm in **b** and c, 50 µm in **b′** and **c′**, 20 µm in **b″**, **c″**, and **d**, and 10 µm in **e**

GFP–hCrb2, the ORF of GFP was cloned into an endogenous SalI restriction site in hCrb2 pDONOR201 [39], placing the GFP 130aa upstream of the transmembrane domain. Cloning of GFP into the extracellular fragment of hCrb3a and hCrb3b was described elsewhere [40].

Generation of stick-and-stone antibody

The Sns antibody was generated by injecting chicken with recombinant GST–Sns$_{intra}$ protein purified from *E. coli* (Davids Biotechnology, Regensburg, Germany).
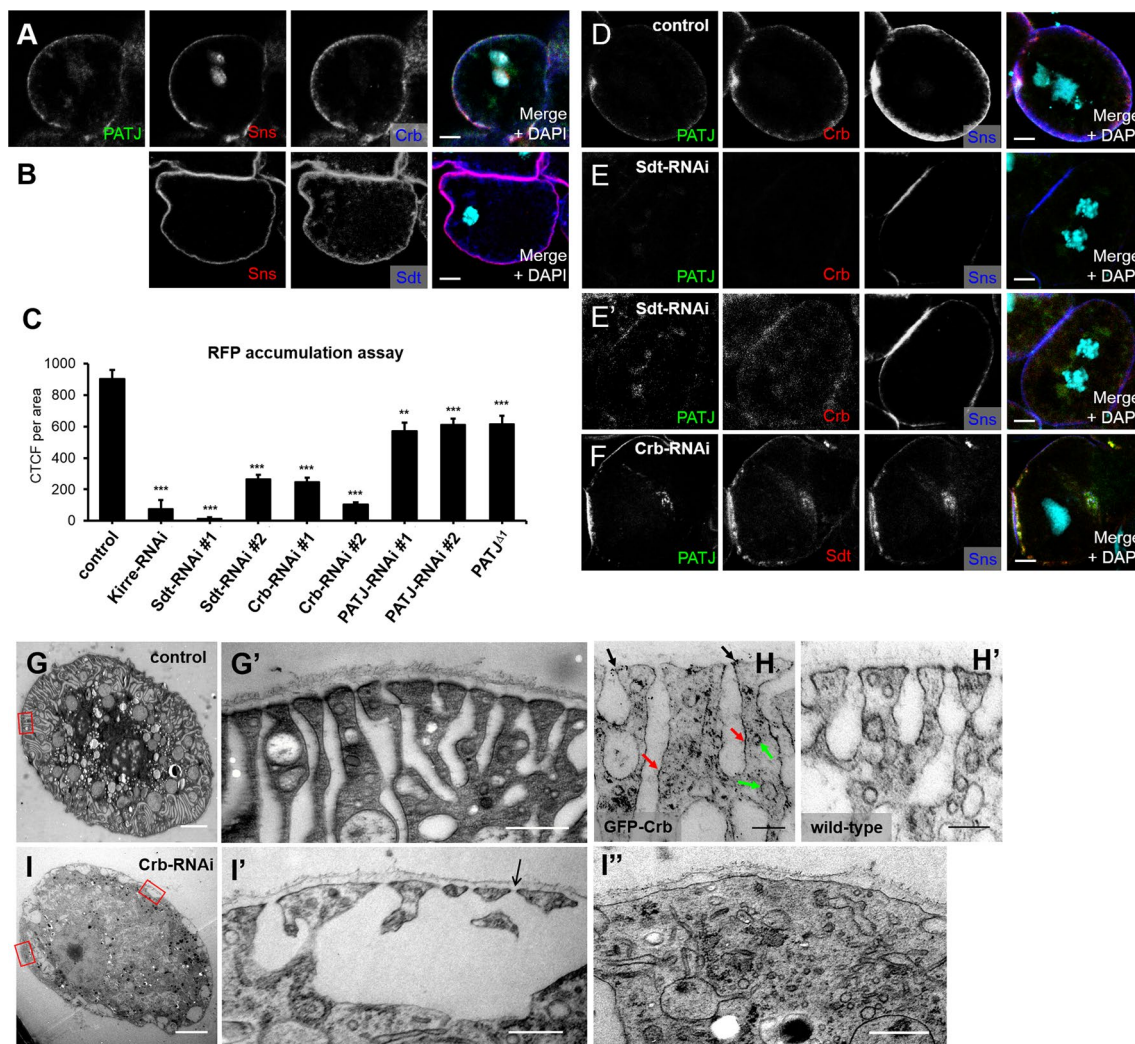
Fig. 2 DmCrb is essential for the function of nephrocytes. **a**, **b** DmCrb, Sdt, and PATJ are expressed in garland nephrocytes and colocalize at the cortex with the Nephrin homologue sticks and stones (Sns). **c** Accumulation of secreted RFP in garland nephrocytes was quantified. All RNAi lines were specifically expressed in nephrocytes using sns::GAL4. An RNAi line against mCherry was used as control. As PATJ null flies survive until pupal stages, filtration efficiency was scored in larvae homozygous for *PATJ$^{\Delta 1}$*, which resulted in approximately the same filtration efficiency as the two RNAi lines used. **d**, **e** Nephrocytes with impaired Sdt expression (Sdt–RNAi#1) show loss of Crb, PATJ, and (to some extent) Sns from the cortical region (same settings in **d** and **e**). Note that increased imaging settings give a cortical signal for Sns, but a rather cytosolic or vesicular signal for Crb and Sdt (**e′**). **f** Downregulation of DmCrb by DmCrb–RNAi#1 does not impair localization of PATJ or Sdt, but results in weaker cortical Sns staining. **g–i** Transmission electron micrographs of garland nephrocytes. In wild-type (not shown) or control nephrocytes (**g**), long, regularly aligned foot processes compose a broad peripheral area of the cells, outlining parallel lacunae in between the foot processes, which are sealed with a slit diaphragm. **h** GFP–Crb expressed from its endogenous promoter [74] localizes at the nephrocyte diaphragms (*black arrow*) as well as along the peripheral outline of the lacunae (*red arrows*) and in vesicles close to the cell cortex (*green arrows*). Garland cells of wild-type flies incubated with GFP antibody were used as negative control (**h′**). In nephrocytes with impaired DmCrb expression (**i**), this peripheral area is severely disturbed and surface area with nephrocyte diaphragms is drastically reduced (quantified in Fig. 3j). **i′**, **i″** are higher magnifications from **i** taken from an area with irregular nephrocyte diaphragms (**i′**) or a nephrocyte diaphragm free area (**i″**). *Scale bar* 5 μm in **a**, **b**, and **d–f**, 2 μm in **g** and **i**, 500 nm in **g′**, **i′**, and **i″**, and 200 nm in **h**

ANP–RFP-accumulation assay

Garland cell nephrocytes from wandering third instar larvae were microdissected in HL3.1 saline [41], fixed in 4% PFA in PBS for 1 h, stained with DAPI for 20 min, washed with PBS, and mounted in mowiol. Samples were imaged using an LSM-510 confocal microscope (ZEISS, Jena, Germany) and ANP–RFP accumulation per nephrocyte area (CTCF = corrected total cell fluorescence) was subsequently analyzed and quantified with ImageJ after subtracting the autofluorescent background of dissected larvae. For each genotype, at least 40 nephrocytes of five independent

larvae were quantified. Error bars indicate the standard error of the mean. Significance was determined by unequal two sample *t* test with unequal variances: ns > 0.05, *$p < 0.05$, **$p < 0.01$, ***$p < 0.001$.

Immunohistochemistry

Garland nephrocytes were dissected as described above and heat-fixed for 20 s in boiling heat fix saline (0.03% Triton-X100). Subsequently, nephrocytes were washed three times in PBS + 0.1% Tween 20 and blocked with 1% BSA for 1 h, incubated over night with primary antibodies in PBS + 0.1% Tween 20 + 1% BSA, washed three times, and incubated for 2 h with secondary antibodies. After three washing steps and DAPI staining, nephrocytes were mounted with Mowiol. For staining of F-actin, garland nephrocytes were fixed in 4% PFA in PBS and stained with Phalloidin-Alexa-568 (Molecular Probes).

Primary antibodies used were as follows: mouse anti-Crb (Cq4, 1:50, Development Study Hybridoma Bank, DSHB), rabbit anti-GFP (1:500, sc-8334, Santa Cruz), guinea pig anti-PATJ (1:500 [17]), rabbit anti-Sdt (1:1000, Koch et al., in revision), mouse anti-Sdt (1:20 [42]), and chicken anti-Sns (1:1000, this study). Guinea pig anti-Rab5 (1:2000), rabbit anti-Rab7 (1:2000), and rabbit anti-Rab11 (1:2000) were kindly provided by A. Nakamura [43]. Rabbit anti-Moesin (1:2000) was kindly provided by D. Kiehart [44]. Secondary antibodies conjugated with Alexa 488, Alexa 568, and Alexa 647 (Life technologies) were used at 1:400. Images were taken on a Zeiss LSM 710 Meta confocal microscope and processed using Adobe Photoshop.

Sections of paraffin-embedded human kidney specimen were stained using rabbit anti-Crb2 (1:50, HPA043674, SIGMA) and rabbit anti-Crb3 (1:50, HPA013835, SIGMA). For co-staining of Crb3 with Nephrin, Cryo-sections of mouse kidneys were stained using the following antibodies: rabbit anti-Crb3 (1:50, HPA13835, Sigma) and guinea pig anti-Nephrin (1:50, Acris, #BP5030).

Transmission electron microscopy

Garland nephrocytes of the third instar larvae were microdissected in HL3.1 saline, high-pressure frozen (EM-PACT2, Leica, Wetzlar, Germany), freeze-substituted in acetone/2% OsO_4/5% H_2O/0.25% uranyl acetate (AFS2, Leica, Wetzlar, Germany), and embedded in Epon. For transmission electron microscopy, 70-nm-thick sections were cut using an ultramicrotome (Leica UC6 or UC7, Wetzlar, Germany). For immunostainings of ultrathin sections, freeze substitution was performed in acetone/0.2% OsO_4/5% H_2O/0.25% uranyl acetate and also embedded in Epon. The GFP-fusion protein was stained on 70-nm sections using goat anti-GFP (1:20, 600-101-215, Rockland) and a secondary 6-nm gold-coupled

rabbit-α-goat IgG (dilution 1:20). All samples were imaged with a TEM-902 transmission electron microscope (ZEISS, Jena, Germany).

Results

Crb2 and Crb3 are expressed in mammalian podocytes

To study the function of Crb in podocytes development and slit-diaphragm assembly, we aimed to identify the expression pattern of Crb proteins in this cell type. In contrast to *Drosophila*, mammalian genomes contain three genes encoding Crb proteins: CRB1, CRB2, and CRB3 (Fig. 1a). As expression of Crb1 is restricted to neuronal tissues (and testis), we focused on immunostainings of Crb2 and Crb3 on sections of human kidney tissue. As depicted in Fig. 1b, Crb2 is highly expressed in human podocytes (the visceral layer of Bowman's capsule, arrow head in Fig. 1b″ as well as in endothelial cells surrounding the capillaries (asterisk in Fig. 1b″) and in the squamous epithelial cells of the parietal layer (arrow in Fig. 1b″), whereas epithelial cells of the tubular system are only slightly stained (Fig. 1b), as reported before [29]. In contrast, Crb3 is present in the glomeruli (endothelial cells, podocytes and parietal cells, Fig. 1c″) as well as in tubular epithelial cells (Fig. 1c) and colocalizes with the slit-diaphragm component Nephrin (murine kidney sections, Fig. 1d, e). Loss of Crb3 in mice results in kidney cysts, which emerge from tubular segments of the nephron, whereas most glomeruli seem to be intact [26]. On the other hand, dysfunction of Crb2 has recently been reported to impair slit-diaphragm/foot-process maintenance in zebrafish and mutations in human CRB2 are associated with congenital nephrosis or nephrotic syndrome in patients [29–31]. However, the strong expression of two Crb variants with high similarity of its intracellular domain in podocytes suggests the possibility that these two proteins function (partly) in redundancy. Therefore, we chose *Drosophila* nephrocytes as model system to study the function of Crb in vivo.

DmCrb and Sdt are essential for nephrocyte function and morphology

DmCrb, Sdt, and PATJ are expressed in nephrocytes, partly overlapping with the staining of Sticks-and-stones (Sns), one of the *Drosophila* Nephrin homologues, in the peripheral area, where the nephrocyte diaphragms are assembled [45] (Fig. 2a, b).

To investigate the function of DmCrb in nephrocyte development and filtration efficiency, we performed filtration assays as described previously [36]. In this system, soluble red fluorescence protein (RFP) is secreted into the larval hemolymph, which is subsequently filtrated, endocytosed,

and stored by nephrocytes (an example for the RFP-accumulation assay is described in Suppl. Fig. 1). Thus, intracellular accumulation of RFP in garland nephrocytes of wandering L3 larvae reflects filtration efficiency and endocytosis. Indeed, downregulation of Kirre, one of the *Drosophila* NEPH1 homologues, results in almost abolished filtration efficiency (Fig. 2c).

Downregulation of DmCrb as well as Sdt significantly decreased filtration efficiency (Fig. 2c). This effect is specific for DmCrb and Sdt, because it can be rescued by expression of an RNAi-resistant variant (Fig. 3d). Interestingly, downregulation or knock-out of PATJ in nephrocytes does not reduce RFP filtration to the same extent as downregulation of DmCrb or Sdt (Fig. 2c), suggesting that PATJ is not necessary to stabilize the DmCrb/Sdt complex in nephrocytes, which corresponds to the situation in the embryonic

epidermis and to some extent in cells of the follicular epithelium [17, 19, 20].

Loss of Sdt in epithelia leads to destabilization and endocytosis of DmCrb [13, 46]. Similarly, we observed a strong decrease in DmCrb (and PATJ) staining in nephrocytes with decreased Sdt expression (Fig. 2e, same settings as in d). Importantly, accumulation of the Nephrin homologue sticks-and-stones at the peripheral area appears weaker compared to the control. Enhanced exposure reveals a cytosolic/vesicular staining of DmCrb and PATJ, whereas residual Sns is still cortically localized (Fig. 2e′). In contrast, downregulation of DmCrb does not affect localization of Sdt or PATJ (Fig. 2f, same setting as d), which is in line with previous observations in epithelial cells of the embryonic epidermis, where Sdt and PATJ can be recruited to the apical junction by Bazooka in the absence of Crb [18, 47].
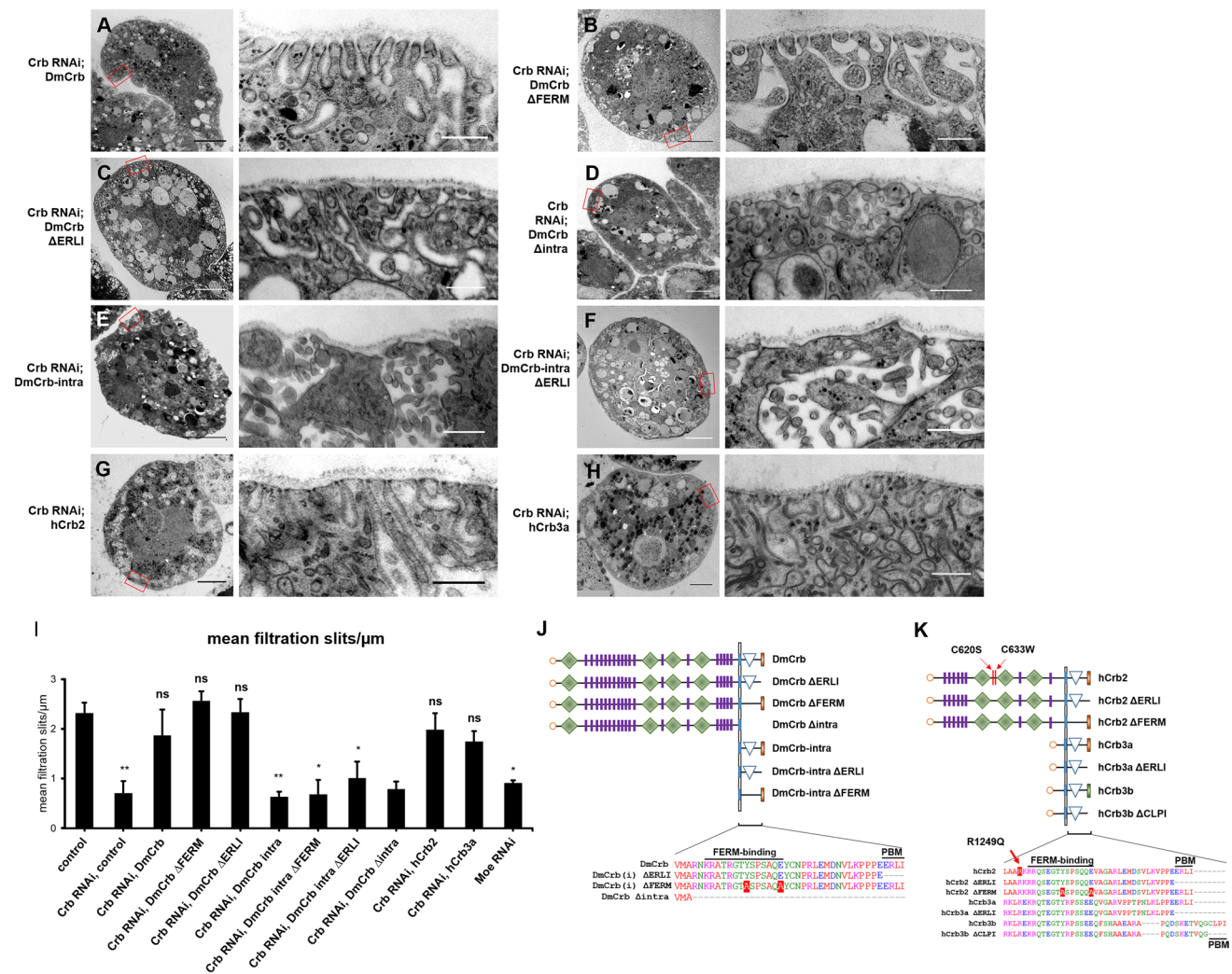
Fig. 3 Transmission electron microscopy analysis of rescue nephrocytes. **a–h** Garland nephrocytes expressing Crb–RNAi and the indicated rescue transgene were analyzed by electron microscopy. **i** Amount of nephrocyte diaphragms (NDs) per μm surface area (basal membrane) was quantified. At least three nephrocytes from different individuals were scored. **j, k** Schematic representation of Crb-deletion constructs and mutations used in this study. *Graphic symbols used are explained in Fig. 1a*

Finally, we investigated whether downregulation of DmCrb affects development and morphology of nephrocytes using electron microscopy. Indeed, formation of foot processes is significantly disturbed in nephrocytes with downregulated DmCrb. In control nephrocytes, the peripheral area is composed of a regularly aligned system of parallel foot processes outlining narrow lacunae, which are sealed to the hemolymph compartment by nephrocyte diaphragms (Fig. 2g). Notably, Crb localizes to the dense structures of nephrocyte diaphragms (Fig. 2h, black arrow), as well to subcortical vesicles (Fig. 2h, green arrow) and around the outline of lacunae (Fig. 2h, red arrow), which is in line with immunostainings (Fig. 2a, d), showing a cortical staining of Crb, which is significantly broader than that of sns (Fig. 2d). In contrast to their control counterparts, nephrocytes with strongly reduced DmCrb protein expression exhibit a dramatically disturbed morphology (Fig. 2i). The peripheral area is irregularly shaped, with a complete loss of correctly aligned foot processes and strongly reduced amount of nephrocyte diaphragms (Fig. 3i). Instead, some big lacunae can be observed, whereas other parts of the cell periphery lack any lacunae. However, some intact nephrocyte diaphragms remain at the border of enlarged lacunae (arrow in Fig. 2i′), which correlates with (reduced but detectable) cortical staining of Sns (Fig. 2f). Morphological defects and amount of nephrocyte diaphragms in Crb–RNAi expressing nephrocytes can be rescued by expression of an RNAi-resistant DmCrb transgene (Fig. 3a, i).

The function of DmCrb regulating nephrocyte diaphragms and RFP accumulation is conserved in its mammalian homologues 2 and 3

Next, we aimed to investigate whether the function of DmCrb in nephrocytes is conserved in mammalian Crb2 and Crb3, which are both expressed in mammalian podocytes (Fig. 1b–e). Human Crb2 (hCrb2) and human Crb3a (hCrb3a) exhibit a high sequence similarity in the cytoplasmic domain, both containing the FERM (4.1-protein–Ezrin–Radixin–Moesin)-binding motif and the C-terminal ERLI motif (Fig. 1a), which is capable of binding the PDZ domain containing proteins Sdt/Pals1 or PAR-6 [12, 13, 15, 25, 48–51]. In contrast to hCrb3a, a second Crb3 isoform, hCrb3b, does not contain the ERLI motif due to alternative splicing [52] (Fig. 1a), and thus, this protein is likely not able to bind Pals1/Sdt. Instead, hCrb3b exhibits a CLPI motif, which has been described to be implicated in ciliogenesis and cell division control [52].

hCrb2 and hCrb3a differ in the extracellular domain, which is quite similar to DmCrb (EGF-like and Laminin A/G-like domains) in case of hCrb2, whereas Crb3a exhibits only a very short extracellular portion (Fig. 1a) which,

however, seems to be sufficient for localization of the protein to cell–cell contacts [40].

To test, which of the human homologues can complement the DmCrb–RNAi phenotypes, we confirmed that overexpressed GFP-tagged hCrb2, GFP–hCrb3a, and GFP–hCrb3b are to some extent colocalizing with DmCrb in the peripheral area of nephrocytes, overlapping with Sns expression (Fig. 4a–c). Notably, overexpression of its mammalian counterparts resulted in a slight expansion of cortical DmCrb localization (Fig. 4a–c, compared to Fig. 2a). Next, we expressed these proteins in nephrocytes together with DmCrb–RNAi. As depicted in Fig. 4d, e, not only RNAi-resistant DmCrb but also hCrb2 and all hCrb3 variants can rescue downregulation of DmCrb regarding the RFP accumulation. Neither deletion of the ERLI motif in hCrb3a (hCrb3a$_{\Delta ERLI}$), nor deletion of the CLPI motif in hCrb3b (hCrb3b$_{\Delta CLPI}$) decreases the rescue capacity of the mutated proteins, but rather results in enhanced filtration (Fig. 4e). Notably, two recently described mutations of hCrb2 (C620S, located within the extracellular domain of hCrb2 between Laminin G domains 1 and 2 and R1249Q, adjacent to the transmembrane domain within the cytoplasmic tail), which are associated with nephrosis [29, 30] rescue downregulation of DmCrb as efficiently as wild-type hCrb2 (Fig. 4d), producing even an increased accumulation of RFP in comparison to control nephrocytes. In contrast, a third mutation (C633W, located in the extracellular domain between Laminin G domains 1 and 2) exhibits only a rescue comparable to control RFP values (Fig. 4d). Considering that these proteins are overexpressed in the rescue experiments, these results might indicate a crucial role of the latter mutation in nephrocyte/podocyte function. However, further experiments using a mammalian system have to be used to elucidate the detailed pathomechanism.

Ultrastructural analysis of hCrb2- and hCrb3a-rescued nephrocytes reveals a complete rescue of morphology and nephrocyte diaphragms (Fig. 3g–i). Thus, both human homologues of DmCrb, which are expressed in human podocytes, are capable of fully accomplishing DmCrb function in nephrocytes regarding filtration efficiency.

The extracellular domain is essential for assembly or maintenance of nephrocyte diaphragms but not for endocytosis

The extracellular domain of DmCrb has been reported to facilitate transcellular homophilic interaction, thereby stabilizing the protein and contributing to DmCrb function in regulating apical–basal polarity in epithelia [53]. Similarly, dimerization of the extracellular domain of two Crb2 isoforms regulates cell adhesion in zebrafish photoreceptor cells [54]. However, expression of a DmCrb variant, which consists of the transmembrane domain and the intracellular
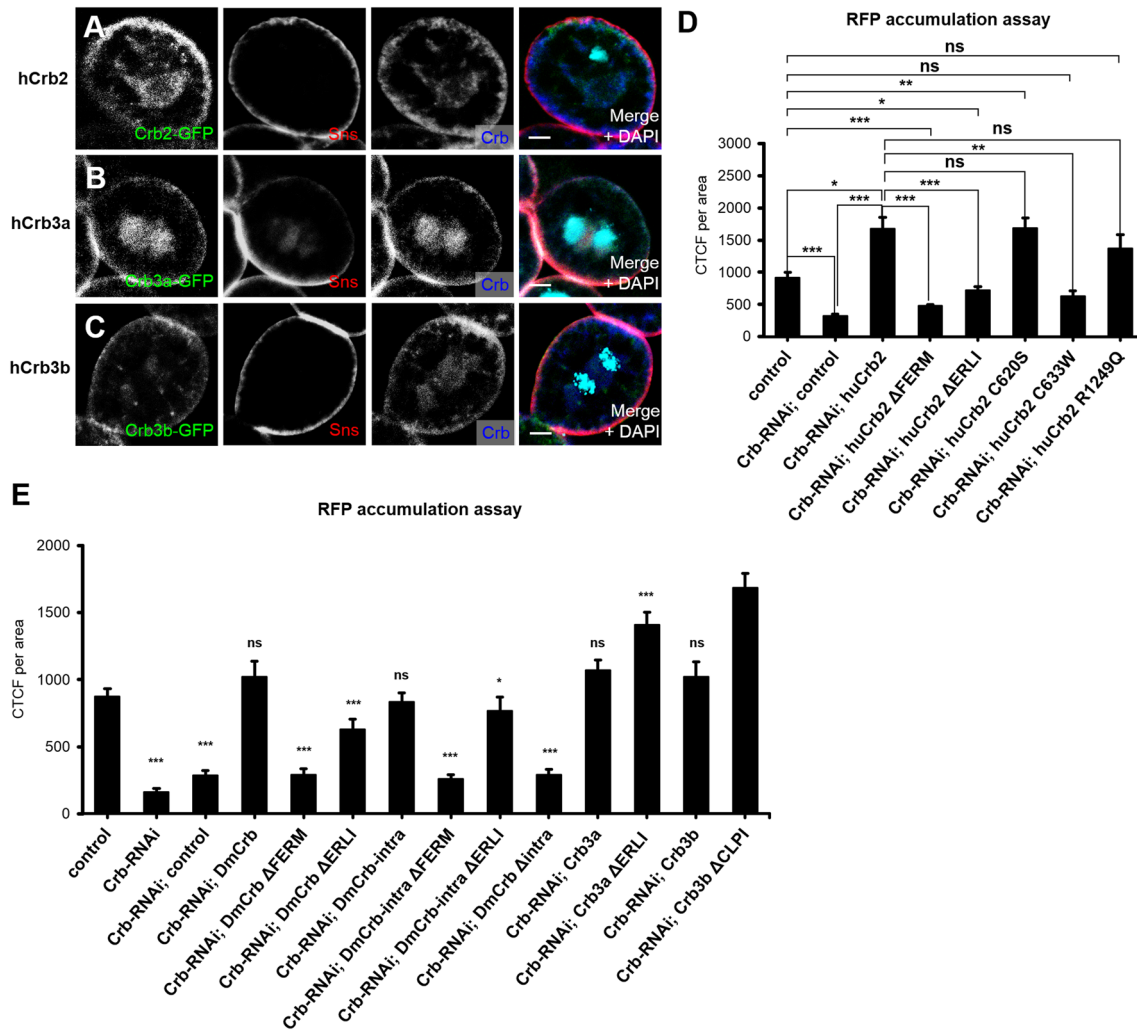
Fig. 4 Crb function for nephrocyte filtration is conserved throughout evolution. **a–c** hCrb2 and hCrb3 isoforms (hCrb3a and hCrb3b, differing at the very C-terminus, as depicted in Fig. 1a) tagged with a GFP (fused into the extracellular domain, next to the transmembrane domain) were expressed in garland nephrocytes and detected by immunostaining. All three hCrb variants colocalize with Sns at the cellular cortex, but show—similar to endogenous DmCrb—an additional subcortical localization. **d, e** Rescue experiments in nephrocytes with downregulated endogenous DmCrb and simultaneous expression of indicated transgenes: accumulation of secreted RFP in garland nephrocytes was quantified as described above. *Scale bars* 5 µm

domain, can at least to some extent restore apical–basal polarity in *crb*-deficient epithelia [38, 55]. This prompted us to test whether homophilic dimerization or other interactions of the extracellular domain of DmCrb are essential for its function in nephrocytes. Indeed, a truncated version of DmCrb (DmCrb_{intra}), consisting only of the signal peptide, the transmembrane domain and the intracellular tail, is able to restore RFP accumulation in nephrocytes with downregulated DmCrb (Fig. 4e).

Remarkably, deletion of the Sdt-interaction motif (ERLI) in this construct does not impair the rescue capacity (Fig. 4e), indicating that Sdt interaction of this motif is not essential for its function in nephrocyte filtration. However, electron microscopy analysis and quantification

of nephrocyte diaphragms indicate a failure in restoring ultrastructure and nephrocyte diaphragms in DmCrb_{intra} and DmCrb_{intraΔERLI} (Fig. 3e, f, i). Thus, rescue potential of the intracellular fragment is likely due to restored/enhanced endocytosis rather than due to nephrocyte diaphragm assembly or maintenance.

In contrast, deletion of the entire cytoplasmic tail in DmCrb (DmCrbΔintra) abolishes the rescue capacity regarding slit-diaphragm assembly (Fig. 3d, i) as well as endocytosis (Fig. 4e), suggesting that the cytoplasmic domain of Crb is essential for these processes, presumably due to targeting of the protein to the cortex/slit diaphragms via interaction with either Sdt (by the ERLI motif) or Moesin (via the FERM-binding motif).

In contrast, hCrb3a exhibits a robust rescue capacity in RFP accumulation as well as in the amount of nephrocyte diaphragms (Figs. 3h, i, 4f), which is in line with a recent study describing a role of the short extracellular domain of Crb3 isoforms in localizing the protein to sites of cell–cell contacts, likely by homophilic interactions [40].

The FERM-binding motif but not the ERLI motif is essential for RFP accumulation

Finally, we elucidated the contribution of the two known intracellular motifs, which are conserved from fly to men: the FERM-binding motif facilitates binding of DmCrb to Yurt, Expanded, and Moesin, thereby modulating the actin cytoskeleton and suppressing cell proliferation and organ growth by controlling the Hippo pathway [56–61].

The C-terminal ERLI motif binds to the adaptor protein Sdt, which is essential for stabilization of Crb at the subapical region in most epithelial cells [12–16], except of boundary cells in the *Drosophila* hindgut [11]. Furthermore, the adaptor protein PAR-6 has been described to compete with Sdt for binding to the ERLI motif of DmCrb and mammalian Crb in vitro and in cell culture [25, 49, 51].

However, the robust rescue capacity of hCrb3b and hCrb3a$_{\Delta ERLI}$ suggests that binding to Pals1/Sdt might not be essential for the filtration efficiency of nephrocytes. Surprisingly, deletion of the ERLI motif in DmCrb (DmCrb$_{\Delta ERLI}$) and hCrb2 (hCrb2$_{\Delta ERLI}$) results in a slightly decreased rescue capacity in comparison to DmCrb, hCrb3b, and hCrb3a$_{\Delta ERLI}$, whereas deletion of the ERLI motif in DmCrb$_{intra}$ does not affect its rescue capacity (Fig. 4d, e). One reason might be that the turnover (by endocytosis) of DmCrb$_{\Delta ERLI}$ could be higher compared to DmCrb, thus disturbing the proteins function at the cell surface. In contrast to the ERLI motif, mutation of the FERM motif (DmCrb$_{\Delta FERM}$ and hCrb2$_{\Delta FERM}$) entirely abolishes the ability to restore DmCrb function regarding nephrocytes filtration efficiency (Fig. 4d, e). Ultrastructural analyses and nephrocyte diaphragm quantifications revealed a close to normal morphology and regular amount of nephrocyte diaphragms in DmCrb$_{\Delta FERM}$ and DmCrb$_{\Delta ERLI}$ (Fig. 3b, c, i). These surprising findings—together with the vice versa effects of DmCrb$_{intra}$—suggest that Crb functions in two pathways to regulate nephrocyte function: The extracellular domain facilitates (presumably by homophilic interaction) nephrocyte diaphragm assembly and/or maintenance and (foot-process) morphology, whereas the intracellular tail (in particular the FERM-binding domain) controls endocytosis (of secreted RFP). Notably, overexpression of DmCrb or its mammalian homologues hCrb2, hCrb3a, and hCrb3b in nephrocytes results in an increased accumulation of RFP (Suppl. Fig. 3), indicating an enhancement of endocytosis, which is in line with previous results, demonstrating a gain of apical membrane compartment upon overexpression of Crb in epithelial cells [55].

Loss of the FERM-binding domain interaction partner Moesin phenocopy Crb-knock-down in nephrocytes

Drosophila nephrocytes accumulate and store filtrated substances upon endocytosis. Interestingly, mammalian podocytes exhibit a similar high endocytosis capacity to regulate slit-diaphragm assembly and maintenance (recently reviewed in Ref. [62]). *Drosophila* nephrocytes endocytose secreted RFP and accumulate it in vesicular structures, which are surrounded by Rab7 staining (but do not costain with Rab5 for early endosomes or Rab11 for recycling endosomes), characterizing them as late endosomes or lysosomes (Fig. 5a and data not shown and Ref. [63]). In contrast to the nephrocyte diaphragm marker Sns (Fig. 2a), DmCrb shows a staining pattern, which is not precisely restricted to the absolute outline of the cell, but exhibits a broader localization (Fig. 2a, d). Furthermore, DmCrb localizes not only to nephrocyte diaphragms, but also to subcortical vesicles and along the outline of lacunae (Fig. 2h). To investigate whether Crb is implicated in the regulation of endocytosis, we stained control and DmCrb-downregulated nephrocytes with markers for early (Rab5) and late endosomes (Rab7). Strikingly, Rab5 and Rab7 staining is dramatically decreased in nephrocytes with downregulated DmCrb (Fig. 4b, same exposure settings as in A, B' shows enhanced settings), reflecting a decrease of early endosomes and late endosomes/lysosomes.

To further explore the mechanism how Crb regulates endocytosis, we analyzed the knock-down phenotypes of the three described interaction partners of the FERM-binding motif: Whereas knock-down of Yurt and Expanded had only a slight decreasing (Yurt) or even enhancing (Expanded) effect on RFP accumulation, reduction of Moesin expression results in a strong reduction of fluorochrome accumulation (Fig. 5c).

Interestingly, knock-down of Moesin in nephrocytes results in a strong decrease in Rab5-positive early endosomes and a substantial decrease in Rab7-positive late endosomes/lysosomes (Fig. 5d), which could be a secondary effect because of the defects in earlier steps of endocytosis. Besides, downregulation of Moesin also affects the actin cytoskeleton, ultrastructure, and the amount of nephrocyte diaphragms (Suppl. Figure 2A–C; Fig. 3i). Downregulation of DmCrb in nephrocytes results in a loss of cortical Moesin (Fig. 6b), which can be rescued by wild-type DmCrb but not by DmCrb$_{\Delta FERM}$ (Fig. 6c, d). Interestingly, downregulation of Moesin in nephrocytes leads to abolished cortical staining of Crb (Suppl. Fig. 2D), indicating that Moesin stabilizes Crb at the cortex, which might explain the morphological defects and reduced nephrocyte diaphragms in Moesin–RNAi expressing nephrocytes.
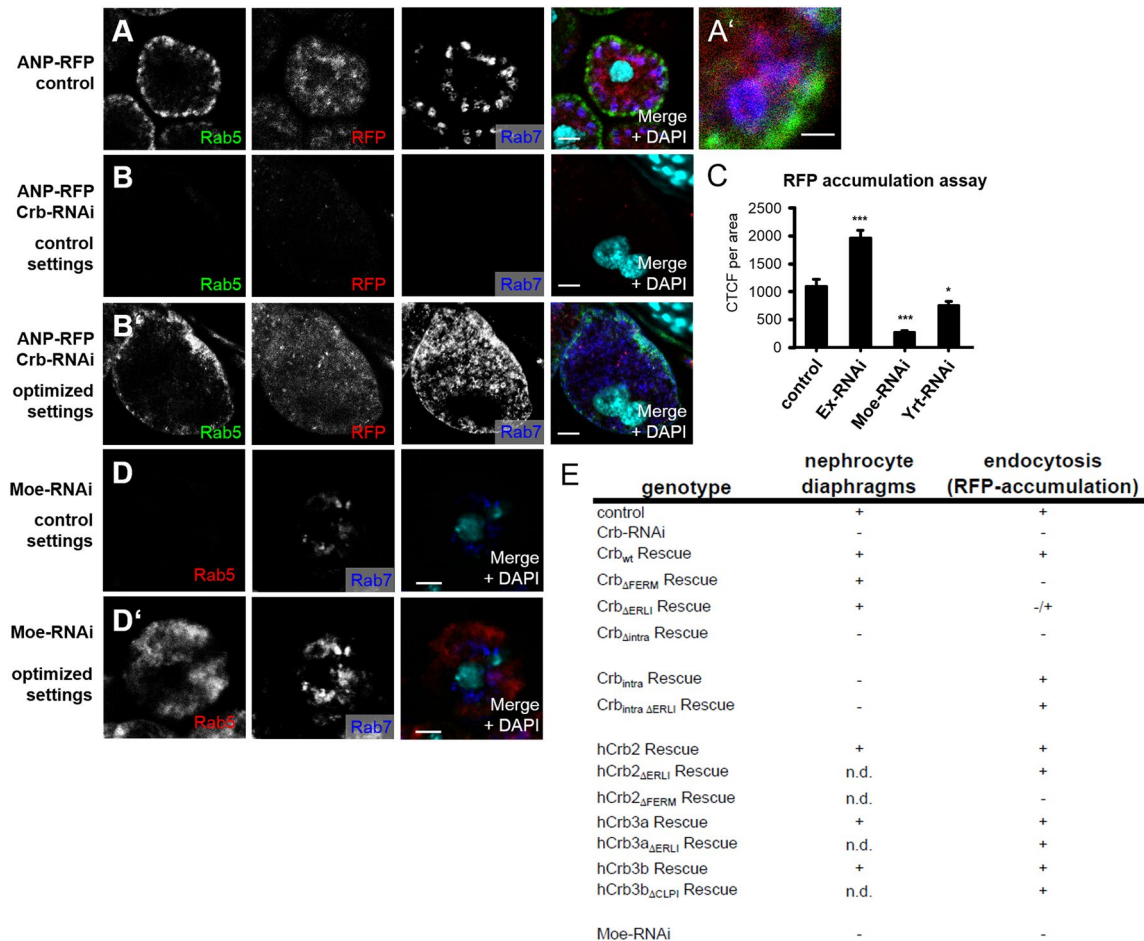
Fig. 5 Crb controls nephrocyte function by regulating endocytosis. **a** Endocytosed RFP accumulates in Rab7-positive vesicles, but does not show overlap with Rab5 (higher magnification in **a′**). **b** Rab7-labeled late endosomes and Rab5-positive early endosomes are decreased in nephrocytes with downregulated DmCrb (**b**, same exposure settings as in **a**, **b′** shows optimized settings) in contrast to control nephrocytes (**a**). **c** RFP-accumulation assay of garland nephrocytes with downregulated expression of Expanded (Ex), Moesin (Moe), or Yurt (Yrt). **d** Nephrocytes expressing Moesin–RNAi show decreased Rab5 and to some extent lower Rab7 staining (same exposure settings as in **a**, **d′** shows optimized settings). **e** Table summarizing the phenotypes observed in nephrocytes with Crb-knock-down and expression of indicated rescue constructs. *Scale bars* 1.5 μm in **a′** and 5 μm in all other

Discussion

Taken together, we have demonstrated that in *Drosophila* nephrocytes, DmCrb regulates early endocytosis by interacting with Moesin via its FERM-binding domain. In contrast, its function in nephrocyte diaphragm assembly/maintenance depends on (presumably homophilic interaction of) the extracellular domain. These two distinct functions are conserved throughout evolution as both mammalian homologues, hCrb2, and both hCrb3 isoforms can rescue the defects observed in nephrocytes with downregulation of DmCrb. Control of endocytosis by Moesin might occur either directly [64, 65] or indirectly by affecting the actin cytoskeleton [66, 67]: Moesin links the Crb apical polarity complex to the actin cytoskeleton in *Drosophila* [57, 61, 68] and mouse Crb3a interacts with a related FERM-domain containing protein, Ezrin, suggesting a similar mechanism [26]. Moreover, Moesin regulates the subcortical actin cytoskeleton and loss of Moesin results in polarity defects [66, 67]. Consequently, downregulation of Moesin disturbs cortical accumulation of DmCrb (Suppl. Fig. 3D), which explains the morphological defects and decreased amount of nephrocyte diaphragms in these cells. On the other hand, Moesin has been described to facilitate the pinching-off of clathrin-coated pits as endocytic vesicles in T cells [64] and in cervix carcinoma cells (HeLa) [65], and thus, it seems to be involved in early steps of endocytosis. Although we provide compelling evidence that Crb regulates endocytosis in nephrocytes by recruiting Moesin via its FERM-binding domain, we cannot exclude that other proteins, which bind directly or indirectly to the FERM-binding motif, are involved in this process, too. Downregulation of Moesin

Fig. 6 Cortical Moesin localization depends on the FERM domain of Crb. **a** In control garland nephrocytes, Moesin localizes in a *dotted* pattern at the cell cortex. **b** Nephrocytes with decreased Crb expression show a decreased cortical Moesin accumulation (**b**), which is diffusely distributed within the cell. **c, d** Wild-type DmCrb but not DmCrb$_{\Delta FERM}$ rescues cortical Moesin localization. *Scale bars* 5 μm
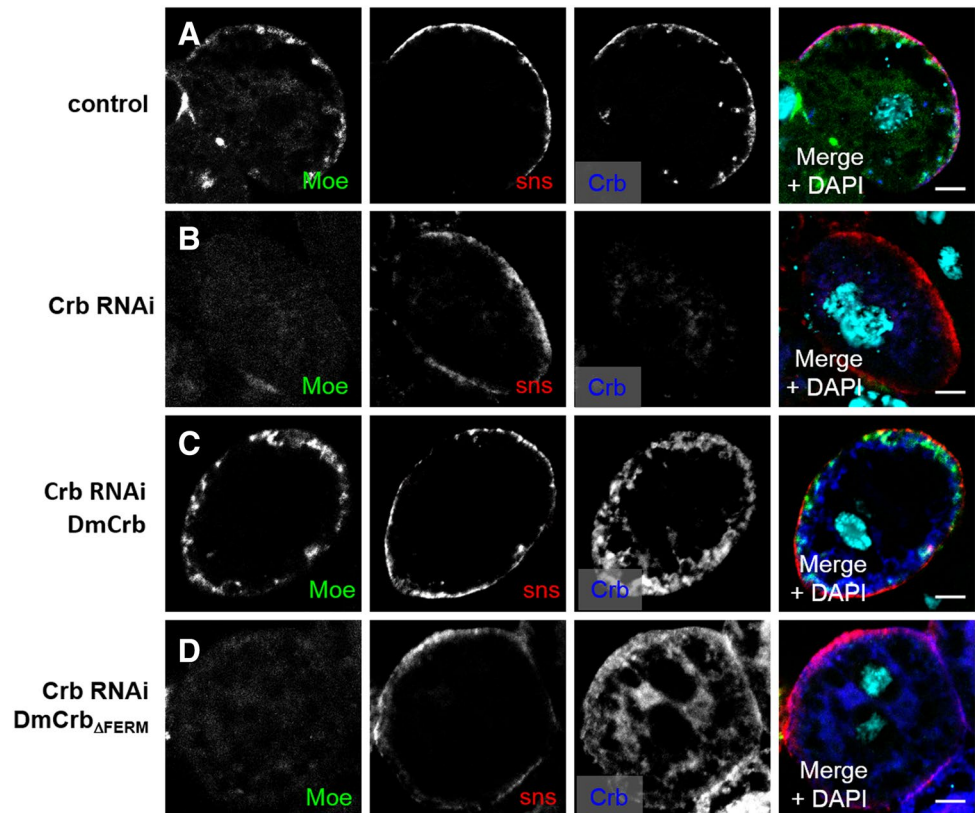
results in severe morphological defects and a strong reduction of nephrocyte diaphragms. In contrast, DmCrbΔFERM rescues nephrocyte morphology and diaphragms but not endocytosis. Thus, we conclude that the Crb–Moesin interaction is essential for regulation of endocytosis, but Moesin accomplishes independently of its recruitment by Crb another function in regulating cell morphology and nephrocyte diaphragm assembly, presumably by modulating the actin cytoskeleton.

Notably, hCrb3a without the ERLI motif and hCrb3b without the CLPI motif as well as hCrb2 are capable of rescuing DmCrb–RNAi nephrocytes more efficiently compared to DmCrb or DmCrbintra (Fig. 4d, e). This is in line with the fact that expression of hCrb2 and hCrb3b but not of hCrb3a in wild-type nephrocytes increased the endocytosis rate more efficiently than DmCrb (Suppl. Fig. 3). Although being highly conserved, the cytoplasmic tails of DmCrb, hCrb2, and hCrb3 isoforms differ in a few amino acids. Thus, fine-tuned differences in the interaction of these proteins with Moesin (or other proteins regulating endocytosis) might produce these differences. Apart from that, it might also be just a matter of either protein stability or protein mobility, which might be increased in proteins without Sdt binding (ΔERLI variants). However, the latter is obviously not the case for the "bigger" Crb proteins DmCrb and hCrb2, because in these cases, the RFP accumulation is weaker upon deletion

of the Sdt-interaction motif. In contrast, the rescue capacities of Crb3 variants without the Sdt-interaction motif are similar or even increased. One explanation would be that in the absence of Sdt binding, hCrb3 is not as fast removed from the membrane as DmCrb or hCrb2.

Importantly, endocytosis of core components of the slit diaphragm in mammalian podocytes plays a crucial role in maintaining the filtration barrier (reviewed in [69]): Nephrin is endocytosed by clathrin-dependent [70] and independent [71] endocytosis. Damaged podocytes in patients, which suffer from nephrotic syndrome, exhibit an increase in the amount of endocytic vesicles and decreased Nephrin surface localization. On the other hand, defects in maturation of endocytic vesicles result in disturbed morphology of podocytes with vacuoles and loss of foot processes and slit diaphragms [72, 73]. These results reflect an important role of the endocytic machinery in development and function of podocytes, which are in line with our findings of a conserved role of Crb-regulating nephrocyte development and function by modulating endocytosis.

References

1. Patrakka J, Tryggvason K (2007) Nephrin—a unique structural and signaling protein of the kidney filter. Trends Mol Med 13(9):396–403. doi:10.1016/j.molmed.2007.06.006

2. Fukasawa H, Bornheimer S, Kudlicka K, Farquhar MG (2009) Slit diaphragms contain tight junction proteins. J Am Soc Nephrol 20(7):1491–1503. doi:10.1681/ASN.2008101117

3. Itoh M, Nakadate K, Horibata Y, Matsusaka T, Xu J, Hunziker W, Sugimoto H (2014) The structural and functional organization of the podocyte filtration slits is regulated by Tjp1/ZO-1. PLoS One 9(9):e106621. doi:10.1371/journal.pone.0106621

4. Huber TB, Schmidts M, Gerke P, Schermer B, Zahn A, Hartleben B, Sellin L, Walz G, Benzing T (2003) The carboxyl terminus of Neph family members binds to the PDZ domain protein zonula occludens-1. J Biol Chem 278(15):13417–13421. doi:10.1074/jbc.C200678200

5. Hartleben B, Schweizer H, Lubben P, Bartram MP, Moller CC, Herr R, Wei C, Neumann-Haefelin E, Schermer B, Zentgraf H, Kerjaschki D, Reiser J, Walz G, Benzing T, Huber TB (2008) Neph-Nephrin proteins bind the Par3–Par6-atypical protein kinase C (aPKC) complex to regulate podocyte cell polarity. J Biol Chem 283(34):23033–23038. doi:10.1074/jbc.M803143200

6. Hirose T, Satoh D, Kurihara H, Kusaka C, Hirose H, Akimoto K, Matsusaka T, Ichikawa I, Noda T, Ohno S (2009) An essential role of the universal polarity protein, aPKClambda, on the maintenance of podocyte slit diaphragms. PLoS One 4(1):e4194. doi:10.1371/journal.pone.0004194

7. Huber TB, Hartleben B, Winkelmann K, Schneider L, Becker JU, Leitges M, Walz G, Haller H, Schiffer M (2009) Loss of podocyte aPKClambda/iota causes polarity defects and nephrotic syndrome. J Am Soc Nephrol 20(4):798–806. doi:10.1681/ASN.2008080871

8. Satoh D, Hirose T, Harita Y, Daimon C, Harada T, Kurihara H, Yamashita A, Ohno S (2014) aPKClambda maintains the integrity of the glomerular slit diaphragm through trafficking of nephrin to the cell surface. J Biochem 156(2):115–128. doi:10.1093/jb/mvu022

9. Hartleben B, Widmeier E, Suhm M, Worthmann K, Schell C, Helmstadter M, Wiech T, Walz G, Leitges M, Schiffer M, Huber TB (2013) aPKClambda/iota and aPKCzeta contribute to podocyte differentiation and glomerular maturation. J Am Soc Nephrol 24(2):253–267. doi:10.1681/ASN.2012060582

10. Tepass U (2012) The apical polarity protein network in Drosophila epithelial cells: regulation of polarity, junctions, morphogenesis, cell growth, and survival. Annu Rev Cell Dev Biol 28:655–685. doi:10.1146/annurev-cellbio-092910-154033

11. Kumichel A, Knust E (2014) Apical localisation of crumbs in the boundary cells of the Drosophila hindgut is independent of its canonical interaction partner stardust. PLoS One 9(4):e94038. doi:10.1371/journal.pone.0094038

12. Bachmann A, Schneider M, Theilenberg E, Grawe F, Knust E (2001) Drosophila Stardust is a partner of Crumbs in the control of epithelial cell polarity. Nature 414(6864):638–643

13. Hong Y, Stronach B, Perrimon N, Jan LY, Jan YN (2001) Drosophila Stardust interacts with Crumbs to control polarity of epithelia but not neuroblasts. Nature 414(6864):634–638

14. Makarova O, Roh MH, Liu CJ, Laurinec S, Margolis B (2003) Mammalian Crumbs3 is a small transmembrane protein linked to protein associated with Lin-7 (Pals1). Gene 302(1–2):21–29

15. Roh MH, Fan S, Liu CJ, Margolis B (2003) The Crumbs3–Pals1 complex participates in the establishment of polarity in mammalian epithelial cells. J Cell Sci 116(Pt 14):2895–2906

16. Straight SW, Shin K, Fogg VC, Fan S, Liu CJ, Roh M, Margolis B (2004) Loss of PALS1 expression leads to tight junction and polarity defects. Mol Biol Cell 15(4):1981–1990. doi:10.1091/mbc.E03-08-0620

17. Sen A, Nagy-Zsver-Vadas Z, Krahn MP (2012) Drosophila PATJ supports adherens junction stability by modulating Myosin light chain activity. J Cell Biol 199(4):685–698. doi:10.1083/jcb.201206064

18. Sen A, Sun R, Krahn MP (2015) Localization and function of Pals1-associated tight junction protein in Drosophila is regulated by two distinct apical complexes. J Biol Chem 290(21):13224–13233. doi:10.1074/jbc.M114.629014

19. Penalva C, Mirouse V (2012) Tissue-specific function of Patj in regulating the Crumbs complex and epithelial polarity. Development 139(24):4549–4554. doi:10.1242/dev.085449

20. Zhou W, Hong Y (2012) Drosophila Patj plays a supporting role in apical-basal polarity but is essential for viability. Development 139(16):2891–2896. doi:10.1242/dev.083162

21. Shin K, Straight S, Margolis B (2005) PATJ regulates tight junction formation and polarity in mammalian epithelial cells. J Cell Biol 168(5):705–711

22. Michel D, Arsanto JP, Massey-Harroche D, Beclin C, Wijnholds J, Le Bivic A (2005) PATJ connects and stabilizes apical and lateral components of tight junctions in human intestinal cells. J Cell Sci 118(Pt 17):4049–4057. doi:10.1242/jcs.02528

23. Tepass U (1996) Crumbs, a component of the apical membrane, is required for zonula adherens formation in primary epithelia of Drosophila. Dev Biol 177(1):217–225

24. Uhlen M, Fagerberg L, Hallstrom BM, Lindskog C, Oksvold P, Mardinoglu A, Sivertsson A, Kampf C, Sjostedt E, Asplund A, Olsson I, Edlund K, Lundberg E, Navani S, Szigyarto CA, Odeberg J, Djureinovic D, Takanen JO, Hober S, Alm T, Edqvist PH, Berling H, Tegel H, Mulder J, Rockberg J, Nilsson P, Schwenk JM, Hamsten M, von Feilitzen K, Forsberg M, Persson L, Johansson F, Zwahlen M, von Heijne G, Nielsen J, Ponten F (2015) Proteomics tissue-based map of the human proteome. Science 347(6220):1260419. doi:10.1126/science.1260419

25. Lemmers C, Michel D, Lane-Guermonprez L, Delgrossi MH, Medina E, Arsanto JP, Le Bivic A (2004) CRB3 binds directly to Par6 and regulates the morphogenesis of the tight junctions in mammalian epithelial cells. Mol Biol Cell 15(3):1324–1333

26. Whiteman EL, Fan S, Harder JL, Walton KD, Liu CJ, Soofi A, Fogg VC, Hershenson MB, Dressler GR, Deutsch GH, Gumucio DL, Margolis B (2014) Crumbs3 is essential for proper epithelial development and viability. Mol Cell Biol 34(1):43–56. doi:10.1128/MCB.00999-13

27. Alves CH, Sanz AS, Park B, Pellissier LP, Tanimoto N, Beck SC, Huber G, Murtaza M, Richard F, Sridevi Gurubaran I, Garcia Garrido M, Levelt CN, Rashbass P, Le Bivic A, Seeliger MW, Wijnholds J (2013) Loss of CRB2 in the mouse retina mimics human retinitis pigmentosa due to mutations in the CRB1 gene. Hum Mol Genet 22(1):35–50. doi:10.1093/hmg/dds398

28. Xiao Z, Patrakka J, Nukui M, Chi L, Niu D, Betsholtz C, Pikkarainen T, Vainio S, Tryggvason K (2011) Deficiency in Crumbs homolog 2 (Crb2) affects gastrulation and results in embryonic lethality in mice. Dev Dyn 240(12):2646–2656. doi:10.1002/dvdy.22778

29. Ebarasi L, Ashraf S, Bierzynska A, Gee HY, McCarthy HJ, Lovric S, Sadowski CE, Pabst W, Vega-Warner V, Fang H, Koziell A, Simpson MA, Dursun I, Serdaroglu E, Levy S, Saleem MA, Hildebrandt F, Majumdar A (2015) Defects of CRB2 cause steroid-resistant nephrotic syndrome. Am J Hum Genet 96(1):153–161. doi:10.1016/j.ajhg.2014.11.014

30. Slavotinek A, Kaylor J, Pierce H, Cahr M, DeWard SJ, Schneidman-Duhovny D, Alsadah A, Salem F, Schmajuk G, Mehta L (2015) CRB2 mutations produce a phenotype resembling congenital nephrosis, Finnish type, with cerebral ventriculomegaly and raised alpha-fetoprotein. Am J Hum Genet 96(1):162–169. doi:10.1016/j.ajhg.2014.11.013

31. Ebarasi L, He L, Hultenby K, Takemoto M, Betsholtz C, Tryggvason K, Majumdar A (2009) A reverse genetic screen in the zebrafish identifies crb2b as a regulator of the glomerular filtration barrier. Dev Biol 334(1):1–9. doi:10.1016/j.ydbio.2009.04.017

32. Weavers H, Prieto-Sanchez S, Grawe F, Garcia-Lopez A, Artero R, Wilsch-Brauninger M, Ruiz-Gomez M, Skaer H, Denholm B (2009) The insect nephrocyte is a podocyte-like cell with a filtration slit diaphragm. Nature 457(7227):322–326. doi:10.1038/nature07526

33. Zhuang S, Shao H, Guo F, Trimble R, Pearce E, Abmayr SM (2009) Sns and Kirre, the Drosophila orthologs of Nephrin and Neph1, direct adhesion, fusion and formation of a slit diaphragm-like structure in insect nephrocytes. Development 136(14):2335–2344. doi:10.1242/dev.031609

34. Na J, Sweetwyne MT, Park AS, Susztak K, Cagan RL (2015) Diet-induced podocyte dysfunction in drosophila and mammals. Cell Rep 12(4):636–647. doi:10.1016/j.celrep.2015.06.056

35. Tutor AS, Prieto-Sanchez S, Ruiz-Gomez M (2014) Src64B phosphorylates Dumbfounded and regulates slit diaphragm dynamics: Drosophila as a model to study nephropathies. Development 141(2):367–376. doi:10.1242/dev.099408

36. Zhang F, Zhao Y, Han Z (2013) An in vivo functional analysis system for renal gene discovery in Drosophila pericardial nephrocytes. J Am Soc Nephrol 24(2):191–197. doi:10.1681/ASN.2012080769

37. Groth AC, Fish M, Nusse R, Calos MP (2004) Construction of transgenic Drosophila by using the site-specific integrase from phage phiC31. Genetics 166(4):1775–1782

38. Klebes A, Knust E (2000) A conserved motif in Crumbs is required for E-cadherin localisation and zonula adherens formation in Drosophila. Curr Biol 10(2):76–85

39. Mitsuishi Y, Hasegawa H, Matsuo A, Araki W, Suzuki T, Tagami S, Okochi M, Takeda M, Roepman R, Nishimura M (2010) Human CRB2 inhibits gamma-secretase cleavage of amyloid precursor protein by binding to the presenilin complex. J Biol Chem 285(20):14920–14931. doi:10.1074/jbc.M109.038760

40. Djuric I, Siebrasse JP, Schulze U, Granado D, Schluter MA, Kubitscheck U, Pavenstadt H, Weide T (2016) The C-terminal domain controls the mobility of Crumbs 3 isoforms. Biochem Biophys Acta. doi:10.1016/j.bbamcr.2016.03.008

41. Feng Y, Ueda A, Wu CF (2004) A modified minimal hemolymph-like solution, HL3.1, for physiological recordings at the neuromuscular junctions of normal and mutant Drosophila larvae. J Neurogenet 18(2):377–402. doi:10.1080/01677060490894522

42. Berger S, Bulgakova NA, Grawe F, Johnson K, Knust E (2007) Unraveling the genetic complexity of Drosophila stardust during photoreceptor morphogenesis and prevention of light-induced degeneration. Genetics 176(4):2189–2200

43. Tanaka T, Nakamura A (2008) The endocytic pathway acts downstream of Oskar in Drosophila germ plasm assembly. Development 135(6):1107–1117. doi:10.1242/dev.017293

44. Edwards KA, Demsky M, Montague RA, Weymouth N, Kiehart DP (1997) GFP-moesin illuminates actin cytoskeleton dynamics in living tissue and demonstrates cell shape changes during morphogenesis in Drosophila. Dev Biol 191(1):103–117. doi:10.1006/dbio.1997.8707

45. Tepass U, Knust E (1990) Phenotypic and developmental analysis of mutations at the crumbs locus, a gene required for the development of epithelia in *Drosophila melanogaster*. Roux's Arch Dev Biol 199:189–206

46. Lin YH, Currinn H, Pocha SM, Rothnie A, Wassmer T, Knust E (2015) AP-2-complex-mediated endocytosis of Drosophila Crumbs regulates polarity by antagonizing Stardust. J Cell Sci 128(24):4538–4549. doi:10.1242/jcs.174573

47. Krahn MP, Buckers J, Kastrup L, Wodarz A (2010) Formation of a Bazooka–Stardust complex is essential for plasma membrane polarity in epithelia. J Cell Biol 190(5):751–760. doi:10.1083/jcb.201006029

48. Roh MH, Makarova O, Liu CJ, Shin K, Lee S, Laurinec S, Goyal M, Wiggins R, Margolis B (2002) The Maguk protein, Pals1, functions as an adapter, linking mammalian homologs of Crumbs and Discs Lost. J Cell Biol 157(1):161–172

49. Kempkens O, Medina E, Fernandez-Ballester G, Ozuyaman S, Le Bivic A, Serrano L, Knust E (2006) Computer modelling in combination with in vitro studies reveals similar binding affinities of Drosophila Crumbs for the PDZ domains of Stardust and DmPar-6. Eur J Cell Biol 85(8):753–767

50. Wang Q, Hurd TW, Margolis B (2004) Tight junction protein Par6 interacts with an evolutionarily conserved region in the amino terminus of PALS1/stardust. J Biol Chem 279(29):30715–30721

51. Whitney DS, Peterson FC, Kittell AW, Egner JM, Prehoda KE, Volkman BF (2016) Crumbs binding to the Par-6 CRIB-PDZ module is regulated by Cdc42. Biochemistry. doi:10.1021/acs.biochem.5b01342

52. Fan S, Fogg V, Wang Q, Chen XW, Liu CJ, Margolis B (2007) A novel Crumbs3 isoform regulates cell division and ciliogenesis via importin beta interactions. J Cell Biol 178(3):387–398. doi:10.1083/jcb.200609096

53. Letizia A, Ricardo S, Moussian B, Martin N, Llimargas M (2013) A functional role of the extracellular domain of Crumbs in cell architecture and apicobasal polarity. J Cell Sci 126(Pt 10):2157–2163. doi:10.1242/jcs.122382

54. Zou J, Wang X, Wei X (2012) Crb apical polarity proteins maintain zebrafish retinal cone mosaics via intercellular binding of their extracellular domains. Dev Cell 22(6):1261–1274. doi:10.1016/j.devcel.2012.03.007

55. Wodarz A, Hinz U, Engelbert M, Knust E (1995) Expression of Crumbs confers apical character on plasma membrane domains of ectodermal epithelia of Drosophila. Cell 82(1):67–76

56. Laprise P, Beronja S, Silva-Gagliardi NF, Pellikka M, Jensen AM, McGlade CJ, Tepass U (2006) The FERM protein Yurt is a negative regulatory component of the Crumbs complex that controls epithelial polarity and apical membrane size. Dev Cell 11(3):363–374. doi:10.1016/j.devcel.2006.06.001

57. Medina E, Williams J, Klipfell E, Zarnescu D, Thomas G, Le Bivic A (2002) Crumbs interacts with moesin and beta(Heavy)-spectrin in the apical membrane skeleton of Drosophila. J Cell Biol 158(5):941–951. doi:10.1083/jcb.200203080

58. Grzeschik NA, Parsons LM, Allott ML, Harvey KF, Richardson HE (2010) Lgl, aPKC, and Crumbs regulate the Salvador/Warts/Hippo pathway through two distinct mechanisms. Curr Biol 20(7):573–581. doi:10.1016/j.cub.2010.01.055

59. Chen CL, Gajewski KM, Hamaratoglu F, Bossuyt W, Sansores-Garcia L, Tao C, Halder G (2010) The apical-basal cell polarity determinant Crumbs regulates Hippo signaling in Drosophila. Proc Natl Acad Sci USA 107(36):15810–15815. doi:10.1073/pnas.1004060107

60. Robinson BS, Huang J, Hong Y, Moberg KH (2010) Crumbs regulates Salvador/Warts/Hippo signaling in Drosophila via the

FERM-domain protein Expanded. Curr Biol 20(7):582–590. doi:10.1016/j.cub.2010.03.019

61. Sherrard KM, Fehon RG (2015) The transmembrane protein Crumbs displays complex dynamics during follicular morphogenesis and is regulated competitively by Moesin and aPKC. Development 142(10):1869–1878. doi:10.1242/dev.115329

62. Inoue K, Ishibe S (2015) Podocyte endocytosis in the regulation of the glomerular filtration barrier. Am J Physiol Renal Physiol 00136:02015. doi:10.1152/ajprenal.00136.2015

63. Soukup SF, Culi J, Gubb D (2009) Uptake of the necrotic serpin in *Drosophila melanogaster* via the lipophorin receptor-1. PLoS Genet 5(6):e1000532. doi:10.1371/journal.pgen.1000532

64. Nomachi A, Yoshinaga M, Liu J, Kanchanawong P, Tohyama K, Thumkeo D, Watanabe T, Narumiya S, Hirata T (2013) Moesin controls clathrin-mediated S1PR1 internalization in T cells. PLoS One 8(12):e82590. doi:10.1371/journal.pone.0082590

65. Barroso-Gonzalez J, Machado JD, Garcia-Exposito L, Valenzuela-Fernandez A (2009) Moesin regulates the trafficking of nascent clathrin-coated vesicles. J Biol Chem 284(4):2419–2434. doi:10.1074/jbc.M805311200

66. Karagiosis SA, Ready DF (2004) Moesin contributes an essential structural role in Drosophila photoreceptor morphogenesis. Development 131(4):725–732. doi:10.1242/dev.00976

67. Speck O, Hughes SC, Noren NK, Kulikauskas RM, Fehon RG (2003) Moesin functions antagonistically to the Rho pathway to maintain epithelial integrity. Nature 421(6918):83–87. doi:10.1038/nature01295

68. Wei Z, Li Y, Ye F, Zhang M (2015) Structural basis for the phosphorylation-regulated interaction between the cytoplasmic tail of cell polarity protein crumbs and the actin-binding protein moesin. J Biol Chem 290(18):11384–11392. doi:10.1074/jbc.M115.643791

69. Soda K, Ishibe S (2013) The function of endocytosis in podocytes. Curr Opin Nephrol Hypertens 22(4):432–438. doi:10.1097/MNH.0b013e3283624820

70. Soda K, Balkin DM, Ferguson SM, Paradise S, Milosevic I, Giovedi S, Volpicelli-Daley L, Tian X, Wu Y, Ma H, Son SH, Zheng R, Moeckel G, Cremona O, Holzman LB, De Camilli P, Ishibe S (2012) Role of dynamin, synaptojanin, and endophilin in podocyte foot processes. J Clin Investig 122(12):4401–4411. doi:10.1172/JCI65289

71. Qin XS, Tsukaguchi H, Shono A, Yamamoto A, Kurihara H, Doi T (2009) Phosphorylation of nephrin triggers its internalization by raft-mediated endocytosis. J Am Soc Nephrol 20(12):2534–2545. doi:10.1681/ASN.2009010011

72. Bechtel W, Helmstadter M, Balica J, Hartleben B, Kiefer B, Hrnjic F, Schell C, Kretz O, Liu S, Geist F, Kerjaschki D, Walz G, Huber TB (2013) Vps34 deficiency reveals the importance of endocytosis for podocyte homeostasis. J Am Soc Nephrol 24(5):727–743. doi:10.1681/ASN.2012070700

73. Chen J, Chen MX, Fogo AB, Harris RC, Chen JK (2013) mVps34 deletion in podocytes causes glomerulosclerosis by disrupting intracellular vesicle trafficking. J Am Soc Nephrol 24(2):198–207. doi:10.1681/ASN.2012010101

74. Klose S, Flores-Benitez D, Riedel F, Knust E (2013) Fosmid-based structure-function analysis reveals functionally distinct domains in the cytoplasmic domain of Drosophila crumbs. G3 (Bethesda) 3(2):153–165. doi:10.1534/g3.112.005074